


Experimental investigation of spherical rubber seismic isolation bearings

Conference Paper**Author(s):**

Katsamakas, Antonios A.; Belser, Gabriel; Vassiliou, Michalis F.; Blondet, Marcial; Stojadinovic, Bozidar 

Publication date:

2021-06

Permanent link:

<https://doi.org/10.3929/ethz-b-000491978>

Rights / license:

In Copyright - Non-Commercial Use Permitted

Funding acknowledgement:

803908 - Seismic Testing of 3D Printed Miniature Masonry in a Geotechnical Centrifuge (EC)

EXPERIMENTAL INVESTIGATION OF SPHERICAL RUBBER SEISMIC ISOLATION BEARINGS

Antonios A. Katsamakas¹, Gabriel Belser², M.F. Vassiliou³, M. Blondet⁴, B. Stojadinovic⁵

¹PhD Candidate, Chair of Seismic Design and Analysis, IBK, ETH Zurich
e-mail: katsamakas@ibk.baug.ethz.ch

² MSc student, IBK, ETH Zurich ³ Assistant Professor, Chair of Seismic Design and Analysis, IBK, ETH Zurich ⁴ Professor, Pontificia Universidad Católica del Perú ⁵ Professor, Chair of Structural Dynamics and Earthquake Engineering, IBK, ETH Zurich
{belserg,vassiliou,stojaadinovic}@ibk.baug.ethz.ch
mblondet@pucp.edu.pe}

Abstract

Seismic isolation is a mature and effective method of reducing earthquake-induced building damage. However, applications of this technology are limited to special and important structures, predominantly in the developed world, due to the associated high costs.

An experimental study of a spherical rubber seismic isolator is presented herein. The cost of these devices is sufficiently low that their wide-spread application in low-income countries seems economically viable. Using a closely spaced grid of such spheres may require only a thin, lightly-reinforced diaphragm slab above the isolation level, further reducing construction costs. Avoiding the cost of this extra slab is crucial to make seismically isolated low-rise buildings economically feasible in poor regions of the globe.

The examined seismic isolation bearings are based on rolling, with rubber spheres rolling on concave (spherical) or flat concrete surfaces. Concave concrete surfaces provide restoring force to the isolated structure through gravity. In contrast, in the case of flat concrete surfaces, no restoring force is applied. Rubber spheres offer increased damping and better stress distribution in the contact areas than spheres made using stiffer materials. This work investigated the effects of the geometry of the rolling surface (i.e., flat or concave), the diameter of the rolling sphere (i.e., 50 or 100 mm), and the applied compressive load on the seismic behavior of these isolation bearings. Initially, the rubber isolators were subjected to monotonic uniaxial compression to examine their behavior under vertical loading. Subsequently, cyclic tests were performed to obtain the lateral force-displacement diagram of the isolation system. It was found that the coefficient of rolling friction depends on the axial load, and the diameter of the spheres. The governing parameter for the design of the rubber spheres is not material failure, but excessive compressive deformation that leads to undesirably high rolling friction. Overall, experimental results proved the efficiency of the investigated system in terms of decreasing the inertia forces transmitted to the superstructure.

Keywords: seismic isolation, rolling bearings, cyclic testing, low-cost construction, rubber bearings

1 INTRODUCTION

Seismic isolation [1,2] is a seismic response modification technique, which uncouples the motion of the structure from the ground shaking. This is achieved by placing a low-stiffness or slippery layer at the base of the structure. This elongates the dominant eigenperiod of the structure, reducing the applied accelerations and, thus, the inertial forces. The main drawback is that it leads to increased displacements; however, these displacements are localized at the isolation level, with the interstory drifts maintaining low values. The three key concepts that a seismic isolation scheme should fulfill are: i) Sufficient bearing capacity under vertical (gravity) loads, ii) sufficient flexibility in the horizontal direction to uncouple the motion of the structure from the ground motion, iii) energy dissipation [3]. An important design consideration is that, when seismic isolation is used, the superstructure should be designed to remain essentially elastic. Previous studies [4,5] proved that this is not a conservative design, but a necessity, emerging from the dynamics of base-isolated structures.

Modern applications of rolling seismic isolation systems focused on isolation of precious equipment, where the supported mass is expected to be low. The rolling spheres were mainly made of steel or rubber, and the supporting plates were made of concrete or steel [6-10]. The geometry of the supporting plates was either conical or concave, providing restoring force through gravity. Even though the efficiency of isolation devices is acknowledged, the implementation of these technologies is limited due to the associated high cost. The high cost originates from a) the cost of the isolation devices and b) the cost of the extra slab required at the isolation level. Finally, the high weight of these devices (can reach 1 ton per device) demands the use of lifting equipment, further increasing the complexity of the construction [11]. There have been numerous attempts to reduce the cost of seismic isolation devices [12-27, among others].

This work focuses on the recently published work by Cilsalar and Constantinou [28-30], who essentially suggested a Friction Pendulum System (FPS bearing) based on rolling instead of sliding (Figure 1). It comprises two concrete surfaces and a stiff rubber sphere (with or without a steel core) that rolls in between. The system is indeed low-cost, as the rubber balls can be obtained for low price. However, it still requires an extra slab above the isolation devices – hence, the overall cost still remains prohibitive for low-rise buildings in low-income countries. This paper suggests the use of a grid of closely-spaced rubber spheres. Using a grid could allow the construction of a thin, lightly reinforced diaphragm, reducing the construction cost (Figure 2). Moreover, since several spheres are used, each sphere supports a lower vertical force (weight); therefore, one could use spheres with smaller diameter, made of rubber material of lower stiffness, and without a steel core.

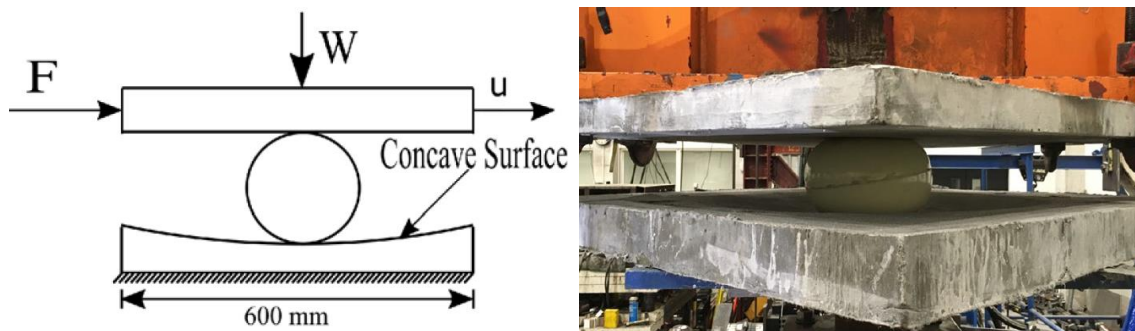


Figure 1: Low-cost rubber rolling isolator, tested by Cilsalar and Constantinou [28-30].

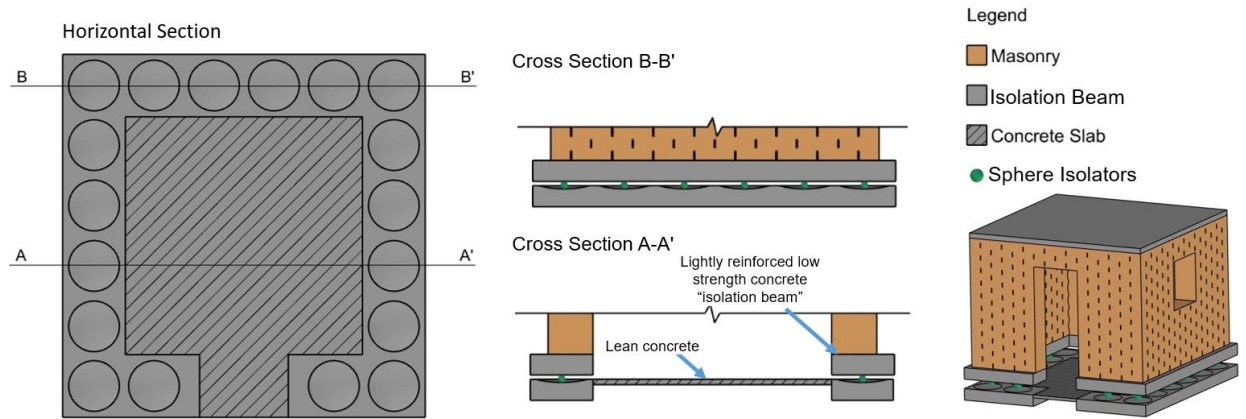


Figure 2: Schematic representation of the low-cost seismic isolation proposed in the present study.

This study presents the compressive and cyclic behavior of low-cost rolling rubber isolators. The cyclic behavior is quantified using a half-scale system of four isolators, capped with a slab. Parameters of investigation are the diameter of the rubber sphere (i.e., 50 mm or 100 mm), the geometry of the concrete plate (i.e., flat or concave), and the supported weight (i.e., 2.08 kN, 3.23 kN or 4.74 kN).

2 EXPERIMENTAL SETUP

2.1 Testing equipment and instrumentation

Cyclic tests were performed using the shake table of the ETH [31] as an actuator. The shake table is a stiff steel box with dimensions of 1 x 2 m, operated by a servo-hydraulic actuator of 100 kN, which acts only in one direction. The stroke, maximum velocity, and maximum payload is 240 mm, 220 mm/second, and 7.5 tons, respectively. Before testing, the accuracy of the shake table was assessed by performing preliminary tests and comparing the applied to the expected motion, with the two being closely correlated.

The experimental setup is shown in Figures 3 and 4. Four isolators (i.e., four pairs of concrete plates) were placed on top of the shake table. A 30mm-thick steel slab was mounted on the top plates, and weight was placed on top of it. The slab was connected to a stiff column via two rigid struts to constrain its motion along the table axis (x) and around the vertical axis (z). Side stoppers and a rail in the middle prevented the slab from moving out of plane. Variable weight in the form of steel beams was placed on top of the structure to apply vertical load on the bearings. In all configurations, the bottom concrete plates were flat. In some configurations, hereafter characterized as “concave,” the top rolling surfaces were spherical.

The plates were made of unreinforced concrete with fine aggregate since steel reinforcement increases cost and construction time, making implementation harder in developing countries. The geometry of the plates is shown in Figure 5.

The radius of curvature of the concave concrete plates (R) was $R = 750$ mm. In plan view, the diameter of the concave concrete plate was 350mm. A commercial low-cost M15 concrete mix was selected, with a maximum aggregate size of 4 mm. The mean compressive and flexural strength was equal to 27.62 MPa, and 4.63 MPa, respectively, tested according to EN 1015-11 (1993) [32]. The utilized rubber spheres were made of natural rubber (NR), with a

shore hardness of 85A. The cost of the 50 mm and 100 mm diameter spheres was 3 \$ and 17\$, respectively [33].

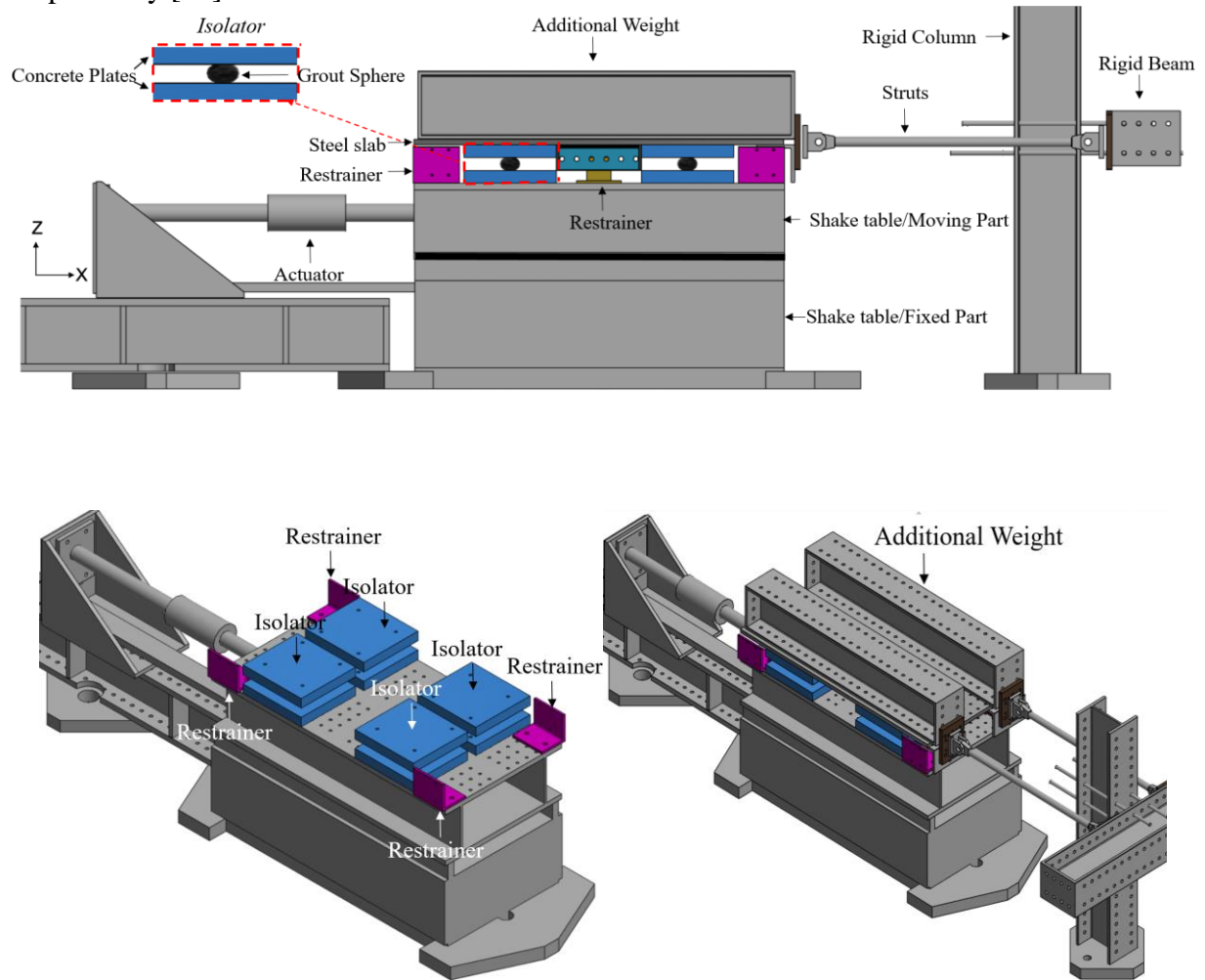


Figure 3: Schematic representation of the utilized experimental setup

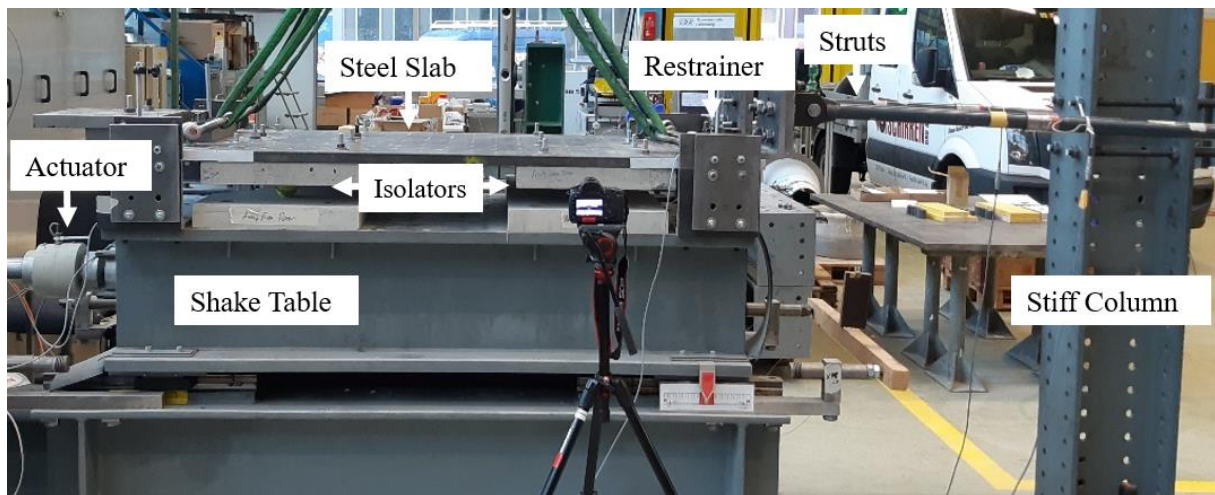


Figure 4: View of the experimental setup

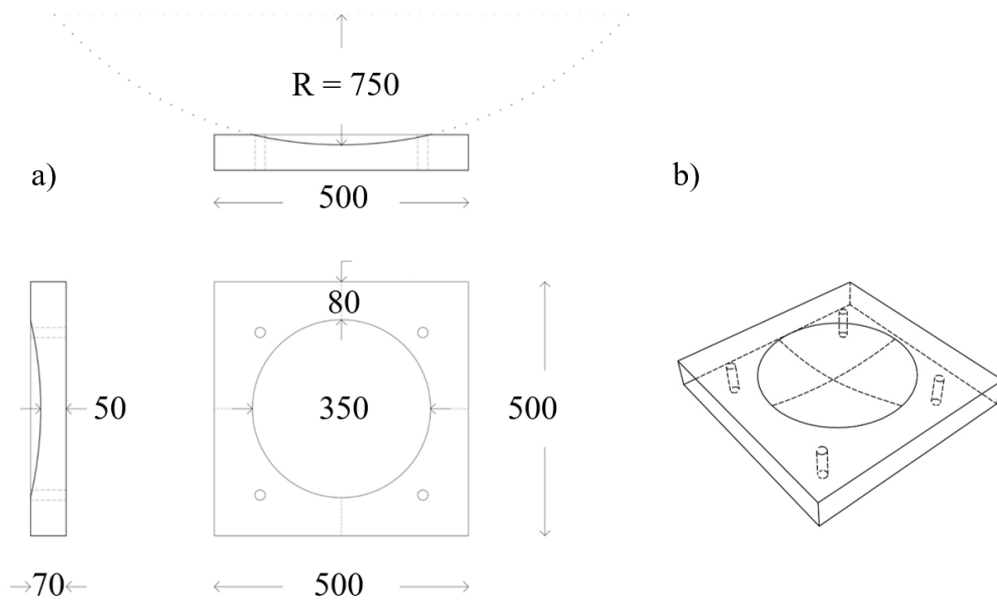


Figure 5: Schematic representation of the utilized concave concrete plates (dimensions in mm); a) Plan and side views, b) 3D view

2.2 Tested configurations and similitude laws

Walls of modern unconfined masonry houses in Cuba weight 2.80 kN/m^2 . Assuming a wall height of 2.8m, gives an unfactored weight of the masonry wall of 7.8 kN/m . A 10 cm roof slab at a typical $5 \times 5 \text{ m}$ room would add 3 kN/m to each wall, giving a total weight of 11 kN/m . Assuming isolators placed every 1 m, the vertical load of each isolator is 11 kN .

The tests were designed assuming a geometrical scaling of $S_L = 1:2 = 0.5$. Therefore, to preserve similitude of stresses the force scaling factor is $S_F = S_L^{-2} = 4$ [34].

Rubber spheres of 50 and 100mm diameter were tested. Three compressive loads (2.08 kN, 3.23 kN or 4.74 kN per sphere in the model scale) under 2 rolling surface geometries (flat/flat and flat/concave) were planned. This corresponds to a total number of 12 configurations. However, due to a limitation of the experimental setup, the spheres with a diameter of 50 mm were tested only with flat concrete plates and with the lower two weight configurations (2.08 kN and 3.23 kN per sphere). A summary of the tested configurations appears in Table 1. Table 2 summarizes the relevant quantities in the model and prototype scale.

Weight per sphere (kN)	Geometry of Concrete Plates	Diameter of Rubber Spheres (mm)	
		100	50
2.08	Flat	Tested	Tested
	Concave	Tested	Not tested
3.23	Flat	Tested	Tested
	Concave	Tested	Not tested
4.74	Flat	Tested	Not tested
	Concave	Tested	Not tested

Table 1: Summary of the tested configurations

Quantity	Model Scale	Prototype Scale
Radius of concave concrete plates	750 mm	1500 mm
Eigenperiod of concave concrete plates	1.74 sec	2.46 sec
Plan view diameter of the concave isolator	350 mm	700 mm
Diameter of large rubber spheres	100 mm	200 mm
Diameter of small rubber spheres	50 mm	100 mm
Vertical load	2.08, 3.23, 4.74 kN	8.32, 12.92, 18.96 kN
Amplitude of cyclic test	± 100 mm	± 200 mm

Table 2: Summary of the main quantities of the experimental model and the corresponding prototype structure

3 TEST RESULTS

3.1 COMPRESSION TESTS

The first part of the experimental investigation comprised monotonic uniaxial compression tests to characterize the response of the rubber spheres under vertical loading (Figure 6). The compression tests were conducted using displacement control. This corresponds to a displacement rate of 0.33 mm/sec and 0.167 mm/sec for the rubber spheres with a diameter of 100 mm and 50 mm, respectively. The compression tests revealed that material failure is not a critical design parameter, since the utilized spheres can sustain very high vertical load, without material failure. The critical design parameter is expected to be the excessive deformation and the associated shape change. Under high vertical loading, the shape of the rolling rubber isolators is no longer spherical; thus, the rolling friction coefficient (i.e., the ratio of horizontal-to-vertical force to initiate rolling) reaches high values.

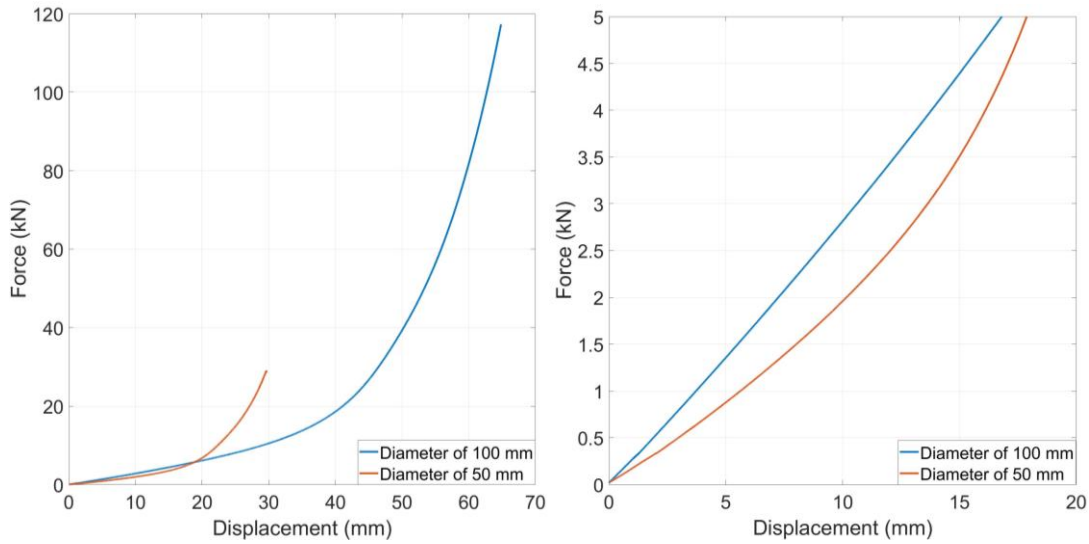


Figure 6. Results of the compression tests of rubber spheres; Left: full view of the tests; Right: Detailed view for the load levels that correspond to the configurations tested in the cyclic tests

3.2 CYCLIC TESTS

The second part of the experimental procedure comprised cyclic testing of the various configurations of rolling isolators. All configurations were subjected to sinusoidal displacement, with an amplitude of 100 mm and a frequency of 0.2 Hz. The isolators were subjected to at

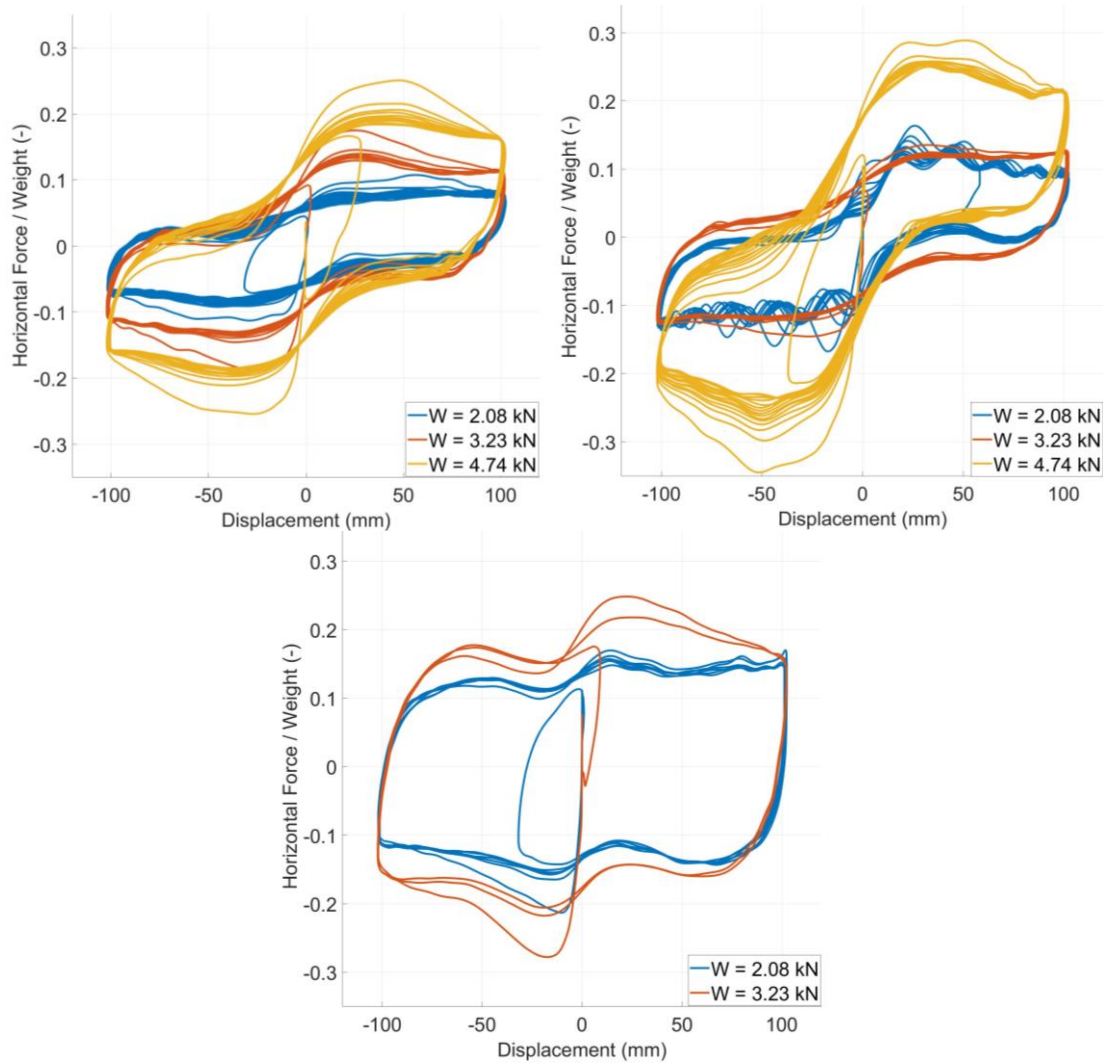


Figure 7. Influence of the vertical load on the cyclic response. Top-left: Spheres with a diameter of 100 mm and flat concrete plates, Top-right: Spheres with a diameter of 100 mm and one concave concrete plate, Bottom: Spheres with a diameter of 50 mm and flat concrete plates

least three cyclic loops, whereas in some cases, more cycles were applied to investigate the possible deterioration of the rolling spheres. All spheres were preloaded for seven days before testing with a load equal to the load they supported during cyclic testing, so that much of their creep is completed.

Figures 7 and 8 present normalized force – deformation loops for different vertical loads. The rolling friction coefficient is defined as $\mu = Q/W$, where Q is the force at zero displacement and W is the weight carried by the bearings. An increase of the vertical load or a reduction of the diameter of the sphere leads to an increased rolling friction coefficient. Moreover, the ratio of the horizontal-to-vertical force increases for all levels of displacement, with the isolation system dissipating more energy (i.e., larger area included in the cyclic loops).

During the first cycle, the spheres exhibit slightly stiffer behavior, whereas after the second cycle, the loop becomes stable, and no further softening is observed. Figure 9 compares the response of flat and concave bearings. Unexpectedly, they exhibit a similar behavior. A possible explanation is that 7 days of creep have resulted in the rubber spheres taking an oval shape that is maintained for the loading rate of the tests. Stiffness originates from the rise of the top plates as the isolator is sheared. It seems that the rise due to the oval shape of the rubber is more important than the one because of the spherical shape of one of the plates. Note,

that the applied displacements cause rotations equal to only 57.3° and 114.6° on the 100mm and 50mm spheres respectively, that is they do not make even half of a full turn. Hence, to explore the behavior at larger displacements, an extrapolation cannot be performed and more tests are needed.

It is worth noting that some cyclic plots include negative-stiffness branches, which are either monotonic or alternating with positive-stiffness branches. These observations are consistent with the observations of Cui et al [6], who tested similar isolators under lower vertical load levels.

Finally, one of the cyclic plots ($W = 2.08$ kN, $D = 100$ mm, Flat concrete plates) demonstrated significant fluctuations, with these fluctuations being consistent over the cycles. Similar behavior has been observed by Nikfar and Konstantinidis [35] in tests of equipment supported on caster tires and is called “flat spotting” and they require further study.

In all cases, the rolling friction coefficient maintained low values, sufficient for seismic isolation applications. A summary of the rolling friction coefficient for each case appears in table 3. The coefficient of friction will be reduced if harder rubber is used.

4 CONCLUSIONS

This paper presents an experimental study on the cyclic and compressive response of low-cost bearings comprising balls rolling on concrete surfaces. Placing the spheres below the walls of the structure at a dense grid would only require the construction of a thin, lightly-reinforced isolation diaphragm, instead of the massive slab that is now required. This is crucial to make seismic isolation affordable in low-income countries.

A half-scale model of prototype bearings was tested, comprising four isolators capped with a slab. Parameters of investigation were the vertical force on each rolling isolator (i.e., 2.08 kN, 3.23 kN, or 4.74 kN), the geometry of the rolling surface (i.e., flat or concave) and the diameter of the rolling sphere (i.e., 50 mm or 100 mm).

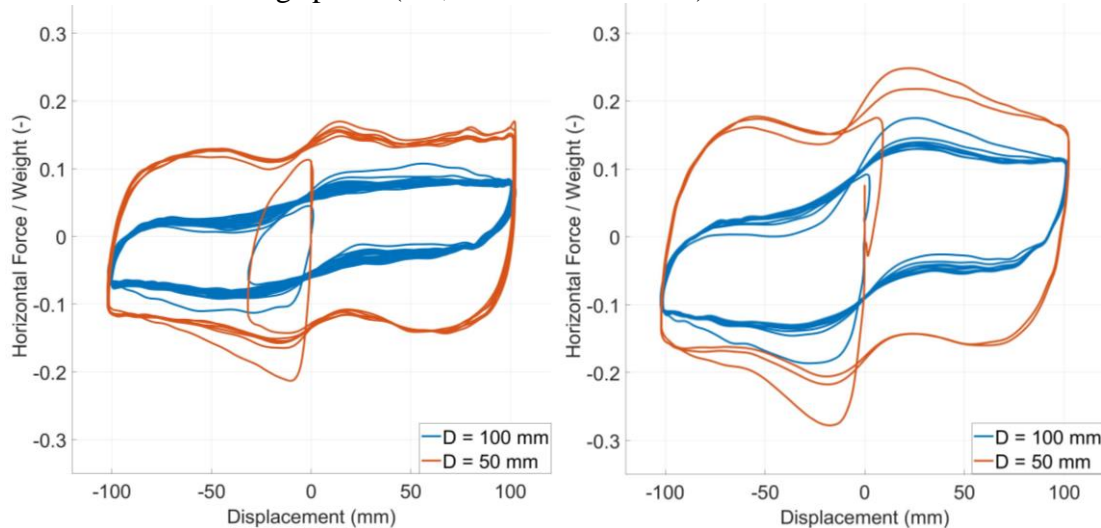


Figure 8. Influence of the diameter of the spheres on the cyclic response, using flat concrete plates. Left: Vertical load of 2.08 kN, Right: Vertical load of 3.23 kN

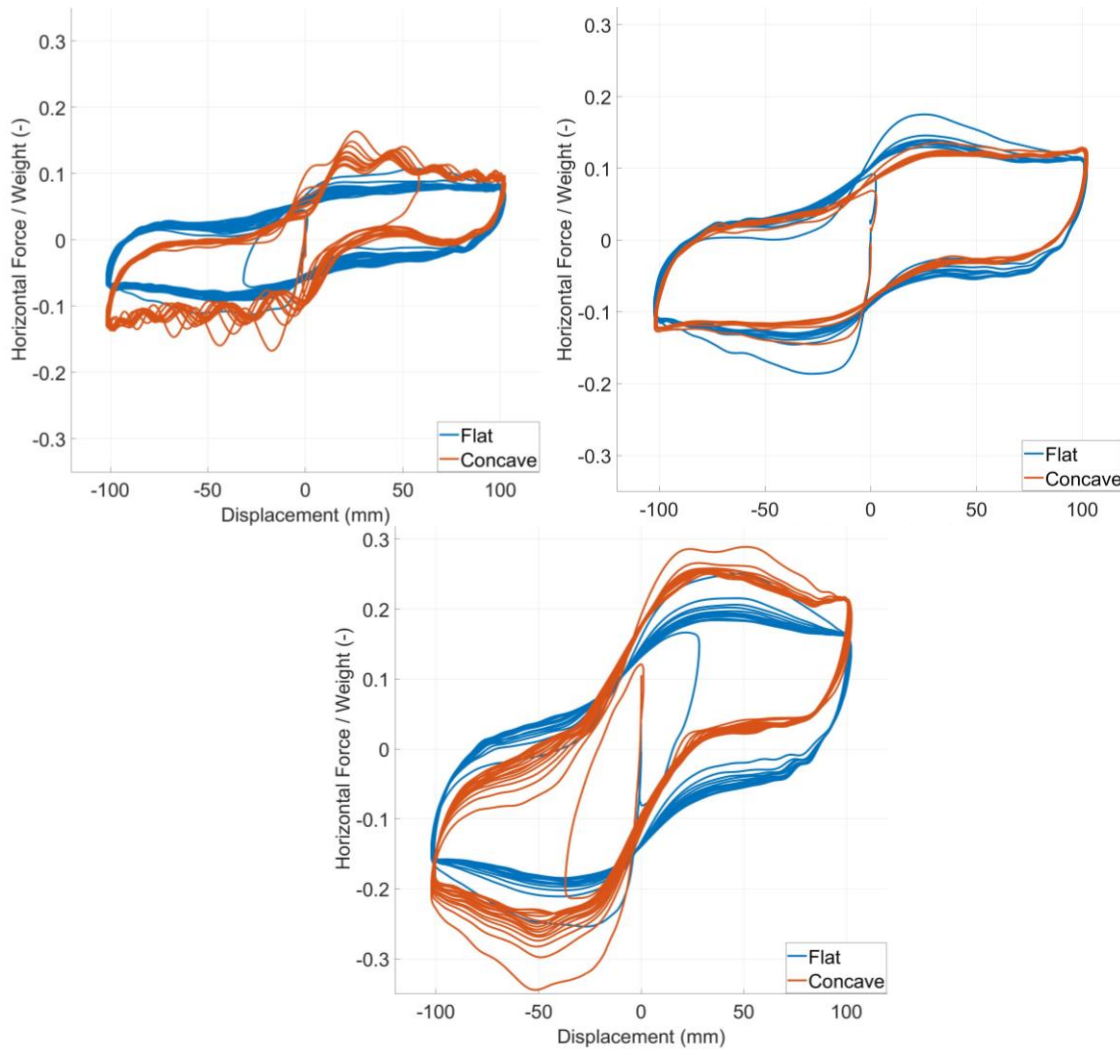


Figure 9. Influence of the geometry of the concrete plates on the cyclic response of spheres with a diameter of 100mm. Top-left: Vertical load of 2.08 kN, Top-right: Vertical load of 3.23 kN, Bottom: Vertical load of 4.74 kN

Diameter of Rubber Sphere (mm)	Vertical Load (kN)	Concrete Plate	Rolling Friction Coefficient (%)
100	2.08	Flat	6.1
		Concave	7.1
	3.23	Flat	8.9
		Concave	8.2
	4.74	Flat	13.7
		Concave	10.7
50	2.08	Flat	13.2
	3.23	Flat	17.6

Table 3: Summary of the rolling friction coefficient of the various tested configurations

Vertical loads up to a representative value for low-rise masonry building in the developing world were applied. Experimental results proved the efficiency of the investigated system in reducing the inertia forces transmitted to the superstructure, with the rolling friction coeffi-

cient (i.e., the ratio of horizontal to vertical force at zero displacement) being in the range of 6.1-17.6 %, thus, suitable for seismic isolation applications.

An increase in the vertical load or a reduction of the size of the sphere leads to a more deformed shape of the isolator, hence, to an increased rolling friction coefficient.

For the displacements considered, the influence of the concrete plate (i.e., flat or concave) is marginal since the deformed shape of the rolling isolator dominates the response. More tests are needed to understand the behavior of the system at larger displacements.

5 ACKNOWLEDGMENT

Support to the first and third author was provided by the European Research Council (ERC) under Starting Grant 803908. The methods, results, opinions, findings, and conclusions presented in this report are those of the authors and do not necessarily reflect the views of the funding agency.

REFERENCES

- [1] Naeim, F., Kelly, J.M. (1999). Design of Seismic Isolated Structures: From theory to practice. John Wiley & Sons
- [2] Kelly, J.M., Konstantinidis, D.A. (2011) Mechanics of Rubber Bearings for Seismic and Vibration Isolation. Wiley
- [3] Makris, N. Seismic isolation: Early history. *Earthquake Engng Struct Dyn.* 2019; 48: 269– 283. <https://doi.org/10.1002/eqe.3124>
- [4] Vassiliou, M.F., Tsiavos, A. and Stojadinović, B. (2013), Dynamics of inelastic base-isolated structures subjected to analytical pulse ground motions. *Earthquake Engng Struct. Dyn.*, 42: 2043-2060. <https://doi.org/10.1002/eqe.2311>
- [5] Tsiavos, A., Mackie, K.R., Vassiliou, M.F., Stojadinovic, B. (2017). Dynamics of inelastic base-isolated structures subjected to recorded ground motions *Bull Earthquake Eng* (2017) 15:1807–1830, DOI 10.1007/s10518-016-0022-5
- [6] Cui, S., Bruneau, M., Constantinou, M.C. (2012) Integrated Design Methodology for Isolated Floor Systems in Single-Degree-of-Freedom Structural Fuse Systems, Technical Report MCEER-12-0004
- [7] Harvey, P.S., Jr., Zéhil, G.-P. and Gavin, H.P. (2014), Experimental validation of a simplified model for rolling isolation systems. *Earthquake Engng Struct. Dyn.*, 43: 1067-1088. <https://doi.org/10.1002/eqe.2387>
- [8] Harvey, P.S., Kelly, K.C. (2016), A review of rolling-type seismic isolation: Historical development and future directions. *Engineering Structures*, Volume 125, 15 October 2016, Pages 521-531, <https://doi.org/10.1016/j.engstruct.2016.07.031>
- [9] Cui S., Bruneau M. (2008) Experimental study of isolated floor systems. *14th World Conference on Earthquake Engineering*
- [10] Foti, D., & Kelly, J. M. (1996). Experimental study of a reduced scale model seismically base isolated with Rubber-Layer Roller Bearings (RLRB). Centre Internacional de Mètodes Numèrics en Enginyeria (CIMNE).

- [11] Kelly JM. (2002) Seismic Isolation Systems for Developing Countries. *Earthquake Spectra*. 2002;18(3):385-406. doi:[10.1193/1.1503339](https://doi.org/10.1193/1.1503339)
- [12] Osgoeei, P.M., Van Engelen, N.C., Konstantinidis, D., Tait, M.J. (2015) Experimental and finite element study on the lateral response of modified rectangular fiber-reinforced elastomeric isolators (MR-FREIs). *Engineering Structures*, <https://doi.org/10.1016/j.engstruct.2014.11.037>
- [13] Osgoeei, P.M., Tait, M.J., Konstantinidis, D. (2014) Three-dimensional finite element analysis of circular fiber-reinforced elastomeric bearings under compression. *Composite Structures*, <https://doi.org/10.1016/j.compstruct.2013.09.008>
- [14] Van Engelen, N. C., Konstantinidis, D., & Tait, M. J. (2016). Structural and nonstructural performance of a seismically isolated building using stable unbonded fiber-reinforced elastomeric isolators. *Earthquake Engineering & Structural Dynamics*, 45(3), 421-439.
- [15] Strauss, A., Apostolidi, E., Zimmermann, T., Gerhaher, U., & Dritsos, S. (2014). Experimental investigations of fiber and steel reinforced elastomeric bearings: Shear modulus and damping coefficient. *Engineering structures*, 75, 402-413.
- [16] Montella, G., Calabrese, A., & Serino, G. (2014). Mechanical characterization of a Tire Derived Material: Experiments, hyperelastic modeling and numerical validation. *Construction and Building Materials*, 66, 336-347.
- [17] Calabrese, A., Spizzuoco, M., Serino, G., Della Corte, G., & Maddaloni, G. (2015). Shaking table investigation of a novel, low-cost, base isolation technology using recycled rubber. *Structural Control and Health Monitoring*, 22(1), 107-122.
- [18] Swensen, S., 2014. Seismically Enhanced Light-Frame Residential Structures, Ph.D. Thesis, Stanford University, Stanford, CA.
- [19] Osgoeei, P.M., Tait, M.J., Konstantinidis, D. (2014) Finite element analysis of unbonded square fiber-reinforced elastomeric isolators (FREIs) under lateral loading in different directions. *Composite Structures*, <https://doi.org/10.1016/j.compstruct.2014.02.033>
- [20] Tran, C., Calabrese, A., Vassiliou, MF., Galano, S. (2020) A simple strategy to tune the lateral response of unbonded Fiber Reinforced Elastomeric Isolators (FREIs). *Engineering Structures*, <https://doi.org/10.1016/j.engstruct.2020.111128>
- [21] Nanda, R.P., Shrikhande. M., Agarwal. P. (2015), Low-cost base-isolation system for seismic protection of rural buildings, *Practice Periodical on Structural Design and Construction (ASCE)* DOI: 10.1061/(ASCE)SC.1943-5576.0000254
- [22] Tsiavos A, Sextos A, Stavridis A, Dietz M, Dihoru L, Alexander NA. (2020) Large-scale experimental investigation of a low-cost PVC ‘sand-wich’ (PVC-s) seismic isolation for developing countries. *Earthquake Spectra*. 2020;36(4):1886-1911. doi:[10.1177/8755293020935149](https://doi.org/10.1177/8755293020935149)
- [23] Tsiavos, A., Alexander, N. A., Diambra, A., Ibraim, E., Vardanega, P. J., Gonzalez-Buelga, A., & Sextos, A. (2019). A sand-rubber deformable granular layer as a low-cost seismic isolation strategy in developing countries: Experimental investigation. *Soil Dynamics and Earthquake Engineering*, 125, 105731.

- [24] Jampole E, Deierlein G, Miranda E, Fell B, Swensen S, Acevedo C. (2016) Full-Scale Dynamic Testing of a Sliding Seismically Isolated Unibody House. *Earthquake Spectra*. 2016;32(4):2245-2270. doi:[10.1193/010616EQS003M](https://doi.org/10.1193/010616EQS003M)
- [25] Das, A., Deb, S. K., & Dutta, A. (2016a). Shake table testing of un-reinforced brick masonry building test model isolated by U-FREI. *Earthquake Engineering & Structural Dynamics*, 45(2), 253-272.
- [26] Van Ngo, T., Dutta, A., & Deb, S. K. (2017). Evaluation of horizontal stiffness of fibre-reinforced elastomeric isolators. *Earthquake Engineering & Structural Dynamics*, 46(11), 1747-1767.
- [27] Das, A., Deb, S. K., & Dutta, A. (2016b). Comparison of Numerical and Experimental Seismic Responses of FREI-Supported Un-reinforced Brick Masonry Model Building. *Journal of Earthquake Engineering*, 20(8), 1239-1262.
- [28] Cilsalar, H., Constantinou, M.C. (2019) Behavior of a spherical deformable rolling seismic isolator for lightweight residential construction. *Bull Earthquake Eng* **17**, 4321–4345 (2019). <https://doi.org/10.1007/s10518-019-00626-z>
- [29] Cilsalar, H., Constantinou, M.C. (2019) Parametric study of seismic collapse performance of lightweight buildings with spherical deformable rolling isolation system. *Bull Earthquake Eng* **18**, 1475–1498 (2020). <https://doi.org/10.1007/s10518-019-00753-7>
- [30] Cilsalar, H., Constantinou, M.C. (2019) Development and Validation of a Seismic Isolation System for Lightweight Residential Construction, Technical Report MCEER-19-0001
- [31] Bachmann H, Wenk T, Baumann M, Lestuzzi P. Der neue ETH-Erdbebensimulator. *Schweizer Ingenieur und Architekt*. 1999;4:63-67.
- [32] EN 1015-11, (1993), “Methods of test for mortar for masonry – Part 11: Determination of flexural and compressive strength of hardened mortar”, European Committee for Standardization, Brussels.
- [33] Xiamen Neway Rubber & Plastic Products Co., Ltd, China, Quotation, February 2020
- [34] Makris, N., & Vassiliou, M. F. (2011). The existence of ‘complete similarities’ in the response of seismic isolated structures subjected to pulse-like ground motions and their implications in analysis. *Earthquake Engineering & Structural Dynamics*, 40(10), 1103-1121.
- [35] Nikfar, F., and Konstantinidis, D. (2017) Shake table investigation on the seismic performance of hospital equipment supported on wheels/casters. *Earthquake Engng Struct. Dyn.*, 46: 243– 266. doi: [10.1002/eqe.2789](https://doi.org/10.1002/eqe.2789).